

# Table-like shape magnetocaloric effect and large refrigerant capacity in dual-phase HoNi/HoNi<sub>2</sub> composite\*

Dan Guo(郭丹), Yikun Zhang(张义坤)<sup>†</sup>, Yaming Wang(王雅鸣), Jiang Wang(王江), and Zhongming Ren(任忠鸣)<sup>‡</sup>

State Key Laboratory of Advanced Special Steels & Shanghai Key Laboratory of Advanced Ferrometallurgy  
& School of Materials Science and Engineering, Shanghai University, Shanghai 200444, China

(Received 12 June 2020; revised manuscript received 11 July 2020; accepted manuscript online 28 July 2020)

Nowadays, magnetic cooling (MC) technology by using the magnetocaloric effect (MCE) has attracted extensive research interest for its promising practical applications. A constant large/giant MCE covers wide refrigeration temperatures (denote as table-like shape) is beneficial for obtaining high efficiency performance for MC. In this paper, the HoNi/HoNi<sub>2</sub> composite was successfully synthesized by arc-melting method and proved to be composed of HoNi and HoNi<sub>2</sub> crystalline phases with weight ratios of 52.4 wt.% and 47.6 wt.%, respectively. The maximum magnetic entropy change ( $-\Delta S_M^{\max}$ ) is 18.23 J/(kg·K), and the refrigerant capacity values  $RC_1$ ,  $RC_2$ , and  $RC_3$  are 867.9 J/kg, 676.4 J/kg, and 467.8 J/kg with  $\Delta H = 0-70$  kOe, respectively. The table-like shape MCE and large refrigerant capacity values make the composite attractive for cryogenic MC using the Ericsson cycle.

**Keywords:** HoNi–HoNi<sub>2</sub> composite, magnetic refrigeration, table-like magnetocaloric effect

**PACS:** 71.20.Eh, 75.30.Sg, 75.30.Cr

**DOI:** 10.1088/1674-1056/aba9be

## 1. Introduction

The magnetic cooling (MC) technology by using the magnetocaloric effect (MCE) has attracted extensive research interests for its promising practical applications. MCE is an inherent property of magnetic solids when changing the external magnetic field.<sup>[1–3]</sup> In the last 30 years, large numbers of researches have focused on searching for the magnetic materials with outstanding MCE due to their environmental-friendly and high cooling efficiency.<sup>[1–5]</sup> To date, many materials were found to exhibit excellent magnetocaloric performances, such as La(Fe,Si)<sub>13</sub>, Gd<sub>5</sub>(SiGe)<sub>4</sub>, Ni–Mn–X, MnFeP<sub>1–x</sub>As<sub>x</sub> as well as some rare-earth (RE) based oxides and compounds.<sup>[4–13]</sup> An important indicator for evaluating the MCE of materials is  $-\Delta S_M$  (magnetic entropy change) and its maximum value is generally corresponding to the transition temperature of the material. Numerous MCE materials with first order magnetic phase transition(s) were found to exhibit large/giant  $-\Delta S_M$  values.<sup>[14–16]</sup> It is well known that the limited operating temperature is a drawback of these materials because of their narrow magnetic phase transition regions, which hinders their practical application. Therefore, extensive efforts were made to explore materials with wider refrigeration temperature region in recent years.

Among the principal cycles used for MC, the Ericsson cycle is considered as an optimal mode, for which the  $-\Delta S_M$  of magnetic materials remaining a constant large value over

a wide refrigeration temperature range (so called table-like shape MCE) is also required.<sup>[17–23]</sup> The parameter of  $RC$  (refrigerant capacity), which is directly connected with the  $-\Delta S_M^{\max}$  and  $\delta T_{FWHM}$  (full-width at half maximum value of  $\Delta S_M-T$  curve), can be used to measure the refrigeration efficiency of magnetic materials. Therefore, the most important thing is to search for materials that achieve constant and temperature-independent  $-\Delta S_M$ . It is difficult to obtain table-like shape MCE in a single-phase material and only a few materials with magnetic field-sensitive magnetic transition or multiple successive magnetic transitions have been reported so far, such as Eu<sub>4</sub>PdMg<sup>[19]</sup> and HoPdIn.<sup>[20]</sup> In contrast, composite materials with two or more materials seem to be easier to achieve table-like shape MCE. Though the table-like MCE was found in some multilayered and powder composites, such as Eu<sub>8</sub>Ga<sub>16</sub>Ge<sub>30</sub>/EuO<sup>[21]</sup> and Fe<sub>87</sub>Zr<sub>6</sub>B<sub>6</sub>Cu<sub>1</sub>/Fe<sub>90</sub>Zr<sub>8</sub>B<sub>2</sub>,<sup>[22]</sup> but some drawbacks (such as poor thermal conductivity, more voids and porosities) in these systems make it a challenge for application. The *in situ* structure composites with different phases in right proportion are more worthy of study, because they do not have such shortcomings and can greatly enhance  $RC$  and obtain a table-like shape MCE. Recently, the dual-phased ErZn<sub>2</sub>/ErZn composites were successfully fabricated by Li *et al.*,<sup>[23]</sup> a table-like shape MCE was obtained with  $-\Delta S_M^{\max}$  of 25.4 J/(kg·K) and large  $RC$  of 645 J/kg under  $\Delta H = 0-70$  kOe.

The RE-Ni system has attracted extensive research in-

\*Project supported by the National Natural Science Foundation of China (Grant No. 51690162), Science and Technology Committee of Shanghai, China (Grant No. 19ZR1418300), Independent Research and Development Project of State Key Laboratory of Advanced Special Steel, Shanghai Key Laboratory of Advanced Ferrometallurgy, Shanghai University (Grant No. SKLASS 2019-Z003), and the Science and Technology Commission of Shanghai Municipality, China (Grant No. 19DZ2270200).

<sup>†</sup>Corresponding author. E-mail: ykzhang@shu.edu.cn

<sup>‡</sup>Corresponding author. E-mail: zmren@shu.edu.cn

terest due to its magnetic properties and hydrogen sorption. On the basis of the phase diagram of Ho–Ni system, eight intermediate phases exist: HoNi, HoNi<sub>2</sub>, HoNi<sub>3</sub>, Ho<sub>3</sub>Ni, Ho<sub>3</sub>Ni<sub>2</sub>, HoNi<sub>5</sub>, Ho<sub>2</sub>Ni<sub>7</sub>, and Ho<sub>2</sub>Ni<sub>17</sub>.<sup>[24]</sup> The HoNi<sub>2</sub> compound which crystallizes in MgCu<sub>2</sub>-type structure was reported to reveal a ferromagnetic (FM) to paramagnetic (PM) phase transition at  $T_C \sim 13.5$  K.<sup>[25]</sup> Several research groups have researched the magnetism of HoNi and two magnetic transitions were found around 13.5 K and 35 K.<sup>[26,27]</sup> Zhou *et al.*<sup>[24]</sup> have reported that three eutectic reactions and seven peritectic reactions can occur in binary Ho–Ni system, among which HoNi and HoNi<sub>2</sub> phases can coexist in the way of eutectic reaction in the range from Ho<sub>60</sub>Ni<sub>40</sub> to Ho<sub>35</sub>Ni<sub>65</sub>. Thus, in this paper, we have fabricated the HoNi–HoNi<sub>2</sub> composite with the nominal composition of Ho<sub>40</sub>Ni<sub>60</sub> and the magnetic properties and MCE performance of this composite were studied.

## 2. Experimental details

The HoNi/HoNi<sub>2</sub> composite was fabricated by directly arc-melting high-purity metals of Ho (99.9%) and Ni (99.95%) with nominal composition of Ho<sub>40</sub>Ni<sub>60</sub> in argon atmosphere. Four times re-melting ensured to achieve a good homogeneity of composition in the arc furnace. Then, the annealing process was conducted at 800 °C for seven days. The phases of HoNi–HoNi<sub>2</sub> composite were confirmed by x-ray diffraction (XRD) using Cu  $K\alpha$  radiation and a 0.02° step size. The FULLPROF software was used to conduct the Rietveld refinement in HoNi–HoNi<sub>2</sub> composite. The microstructure and composition of HoNi–HoNi<sub>2</sub> composite were determined by using a SU8010 scanning electron microscope (SEM) with energy dispersive spectroscopy (EDS) attached. The magnetization data for HoNi–HoNi<sub>2</sub> composite were collected by PPMS-9 with the option of vibrating sample magnetometer (VSM).

## 3. Results and discussion

The XRD pattern as well as Rietveld refinement analyzed by FULLPROF software for HoNi/HoNi<sub>2</sub> composite is described in Fig. 1. The refinement result confirms that the composite contains only HoNi and HoNi<sub>2</sub> phases, which crystallize in orthorhombic FeB-type ( $Pnma$ ) and cubic MgCu<sub>2</sub>-type ( $Fd\bar{3}m$ ) structures, respectively. The weight ratio is fitted to be 52.4 wt.% of HoNi phase and 47.6 wt.% of HoNi<sub>2</sub> phase, which is close to the estimated value with the nominal composition. The obtained Rietveld factors  $R_{wp}$ ,  $R_{exp}$ , and  $\chi^2$  are 8.33%, 6.85%, and 1.48, respectively. The refined lattice parameters are  $a = 7.011(1)$  Å,  $b = 4.143(1)$  Å,  $c = 5.435(4)$  Å, and  $V = 157.868(2)$  Å<sup>3</sup> for HoNi, as well as  $a = 7.149(3)$  Å and  $V = 365.372(5)$  Å<sup>3</sup> for HoNi<sub>2</sub>, which are identical with the values reported in the literatures.<sup>[25,27]</sup> The inset of Fig. 1

shows back-scattered scanning electron (BSE) image of the as-cast HoNi/HoNi<sub>2</sub> composite. It can be found that the microstructure is composed of the grey phase and black phase. The EDS analysis shows that the compositions of the grey phase are 49.91 at.% Ho and 50.09 at.% Ni and those of the black phase are 33.21 at.% Ho and 66.79 at.% Ni, which are determined to be 1 : 1 phase and 1 : 2 phase, respectively.

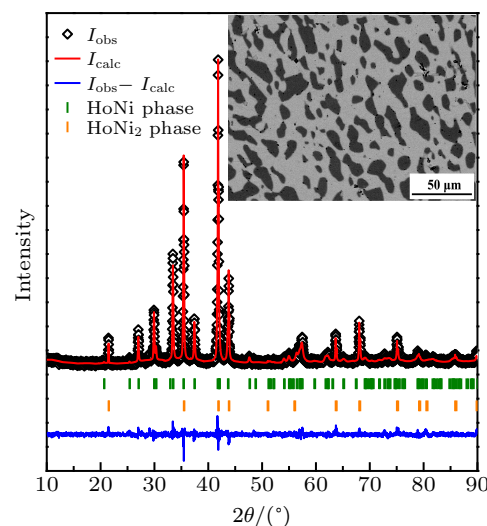
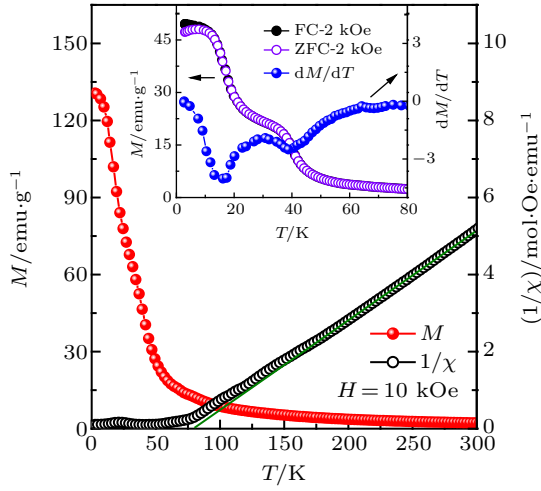
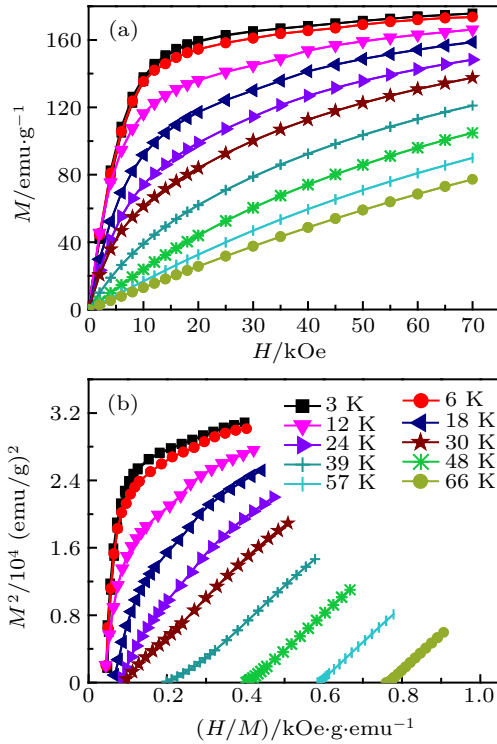


Fig. 1. The XRD pattern of HoNi/HoNi<sub>2</sub> composite along with Rietveld refinement using FULLPROF program. Inset shows the BSE image of HoNi/HoNi<sub>2</sub> composite.

The magnetization  $M(T)$  for the HoNi/HoNi<sub>2</sub> composite measured in zero-field-cooled (ZFC) and field-cooled (FC) modes under a magnetic field  $H = 2$  kOe is displayed in the inset of Fig. 2. A small splitting in FC and ZFC curves is detected at lower temperature, similar behavior can also be found in other materials,<sup>[4,23]</sup> which can probably be ascribed to the pinning effect of domain walls. For higher temperature, the  $M(T)$  curves in both modes are consistent with each other, indicating the absence of thermal hysteresis in HoNi/HoNi<sub>2</sub> composite. Three magnetic transitions are found around 13 K, 16 K, and 38.5 K for HoNi/HoNi<sub>2</sub> composite, which are determined by the  $dM/dT$  vs.  $T$  curve (displayed in the inset of Fig. 2). These temperatures are close to the magnetic phase transition temperatures of HoNi (13.5 K and 35.5 K)<sup>[26]</sup> and HoNi<sub>2</sub> (13.5 K),<sup>[25]</sup> respectively. The slight differences in values could be due to the different preparation processes. The curves of  $M(T)$  and the corresponding reciprocal susceptibility  $1/\chi(T)$  for HoNi–HoNi<sub>2</sub> composite under  $H$  of 10 kOe are shown in Fig. 2. Linearity of  $1/\chi$  can be found in HoNi/HoNi<sub>2</sub> composite in the high temperature region. The paramagnetic Curie temperature  $\theta_p \sim 81.5$  K is obtained by extrapolating the linear part of the  $1/\chi(T)$  curve to abscissa, which confirms that the ground state is ferromagnetic in HoNi–HoNi<sub>2</sub> composite. The effective moment ( $\mu_{eff}$ ) of the HoNi–HoNi<sub>2</sub> composite is  $10.65 \mu_B$ , which is quite near the theoretical value of free Ho<sup>3+</sup> ion ( $10.60 \mu_B$ ) calculated by Hund's rules.<sup>[28]</sup>



**Fig. 2.** The  $T$  dependence of  $M$  (left-scale) and  $1/\chi$  ( $H/M$ , right-scale) at  $H = 10$  kOe for HoNi/HoNi<sub>2</sub> composite. The inset illustrates  $M$ - $T$  curves measured at  $H = 2$  kOe in ZFC and FC modes as well as  $dM/dT$ - $T$  curve for HoNi/HoNi<sub>2</sub> composite.



**Fig. 3.** (a) The  $M$ - $H$  curves under  $H$  up to 70 kOe for HoNi/HoNi<sub>2</sub> composite. (b) The corresponding Arrott-plots ( $M^2$  vs.  $H/M$ ).

Figure 3(a) displays the magnetic isotherms  $M$ - $H$  of HoNi-HoNi<sub>2</sub> composite measured at a series of temperatures up to 70 kOe. At low temperature,  $M$  varies rapidly below  $H = 10$  kOe and then increases slightly and almost saturates under high  $H$ , which is typical performance of FM state. At the temperature of 3 K, the magnetic moment in HoNi/HoNi<sub>2</sub> composite at 70 kOe is estimated to be 7.65  $\mu_B$  per Ho, which is smaller than the theoretical saturation moment  $M_{\text{sat}}$  for Ho<sup>3+</sup> ion (10.0  $\mu_B$ ). It is well known that the 4f shell of rare earths having nonzero orbital angular momentum ( $L \neq 0$ ) and its environment, known as crystalline electric field (CEF), greatly influence the magnetic properties of the rare earth system. Due

to the combined effect of spin-orbit coupling and crystal field, the magnetic anisotropy of the single ion is caused, which reduces the saturation magnetization. Similar phenomena have also been reported in the literatures,<sup>[20,25,26]</sup> i.e., the applied  $H$  of 70 kOe is insufficient to saturate the magnetization of Ho atoms, and a higher  $H$  is needed to overcome the splitting of the CEF to reach the saturated moment. For the temperature above  $T_C$ ,  $M$  increases almost linearly with  $H$ , corresponding to the PM state at these temperatures. No magnetic hysteresis can be found for all  $M$ - $H$  curves, which prompts us to explore the MCE of HoNi-HoNi<sub>2</sub> composite. The Arrott-plots ( $M^2$  vs.  $H/M$ ) are transferred and plotted in Fig. 3(b) to evaluate the orders of phase transitions in HoNi/HoNi<sub>2</sub> composite. Based on Banerjee criterion,<sup>[29]</sup> only positive slope is observed, which confirms that the magnetic phase transitions in HoNi/HoNi<sub>2</sub> composite are second-order ones.

To characterize the MCE of materials, the  $-\Delta S_M$  (magnetic entropy change) is computed based on the magnetization data according to Maxwell thermodynamic relation

$$\begin{aligned} \Delta S_M(T, H) &= S_M(T, H) - S_M(T, 0) \\ &= \int_0^H (\partial M(T, H) / \partial T) H dH. \end{aligned} \quad (1)$$

The magnetization measurement was actually conducted in small discrete magnetic fields and temperature intervals, the values of  $-\Delta S_M$  are computed by the following equation:

$$\begin{aligned} &\Delta S_M [(T_i + T_{i+1}) / 2] \\ &\approx \left[ \int_0^H M(T_i, H) dH - \int_0^H M(T_{i+1}, H) dH \right] / (T_{i+1} - T_i). \end{aligned} \quad (2)$$

Figure 4 displays the  $-\Delta S_M$ - $T$  curves for HoNi/HoNi<sub>2</sub> composite under different  $\Delta H$  from 0–10 kOe to 0–70 kOe. Due to the contributions of phase transitions of HoNi and HoNi<sub>2</sub> phases, two peaks and platform can be found in the  $-\Delta S_M$ - $T$  curves. Partial overlap of the two peaks leads to the occurring of a table-like shape MCE. The maximum  $-\Delta S_M$  ( $-\Delta S_M^{\text{max}}$ ) values of HoNi/HoNi<sub>2</sub> composite are calculated to be 14.93 J/(kg·K) and 18.23 J/(kg·K) for  $\Delta H = 0$ –50 kOe and 0–70 kOe, respectively. Furthermore, the average magnitude of the platform is estimated to be 11.9 J/(kg·K) for  $\Delta H = 0$ –50 kOe and 15.3 J/(kg·K) for  $\Delta H = 0$ –70 kOe, which is competitive with that of other table-like shape MCE materials.

To evaluate the cooling efficiency of MR materials, the parameter  $RC$  is calculated in this paper. Three methods are generally employed to calculate the values of  $RC$ : (i)  $RC_1 = -\Delta S_M^{\text{max}} \times \delta T_{\text{FWHM}}$ ; (ii)  $RC_2 = \int_{T_{\text{cold}}}^{T_{\text{hot}}} |\Delta S_M| dT$ ,  $T_{\text{cold}}$  and  $T_{\text{hot}}$  are temperature points at  $T_{\text{FWHM}}$ ; (iii)  $RC_3$ : the maximum value of the product of  $-\Delta S_M \times \Delta T$  below the  $\Delta S_M$ - $T$  curve. The calculated values of  $RC_1$ ,  $RC_2$  and  $RC_3$  for HoNi-HoNi<sub>2</sub> composite compound are 623.5 J/kg, 469.2 J/kg, and 342.4 J/kg for  $\Delta H = 0$ –50 kOe, to be 867.9 J/kg, 676.4 J/kg,

and 467.8 J/kg for  $\Delta H = 0\text{--}70$  kOe, respectively. Table 1 displays several MCE parameters under  $\Delta H = 0\text{--}50$  kOe for HoNi/HoNi<sub>2</sub> composite to compare with those of other reported compounds as well as some table-like shape MCE materials. We can see that the comparable or even larger values of  $RC_1$  for present HoNi/HoNi<sub>2</sub> composite making it suitable for cryogenic MR using the Ericsson cycle.

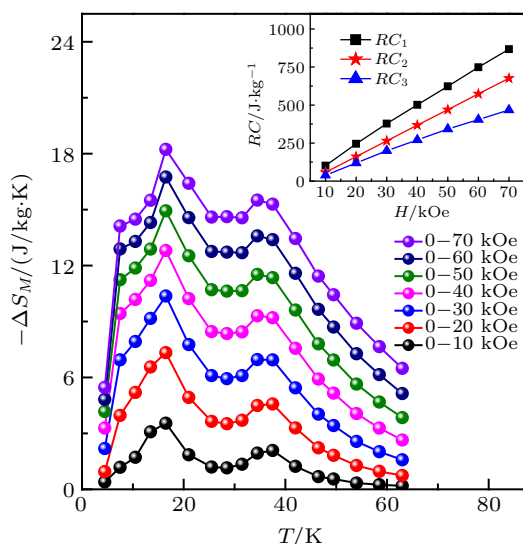


**Fig. 4.** The  $-\Delta S_M$ - $T$  curves at different  $\Delta H$  for HoNi/HoNi<sub>2</sub> composite compound. Inset illustrates the  $RC_1$ ,  $RC_2$ , and  $RC_3$  values at different  $\Delta H$  for HoNi/HoNi<sub>2</sub> composite.

**Table 1.** The  $T_M$ ,  $-\Delta S_M^{\max}$ , and  $RC_1$  for HoNi/HoNi<sub>2</sub> composite and recently reported table-like MCE materials, as well as some other MR materials under the field change of 0–50 kOe.

Materials	$T_M$ /K	$-\Delta S_M^{\max}$ /J·kg <sup>-1</sup> ·K <sup>-1</sup>	$RC_1$ /J·kg <sup>-1</sup>	Ref.
HoNi/HoNi <sub>2</sub>	13/16/38.5	14.93	623.5	this work
HoNi	13.5/35.5	16.6	~ 691	[26]
ErGa	15/30	21.3	~ 658	[17]
0.4(DyNi <sub>2</sub> )+0.6(TbNi <sub>2</sub> )	21.5/37	12.9	526	[18]
HoPdIn	6/23	14.6	496	[20]
ErZn <sub>2</sub> /ErZn	9/20	19.5	447	[23]
GdCo <sub>2</sub> B <sub>2</sub> C	17.2	10.34	238.1	[30]
Ho <sub>3</sub> Pd <sub>2</sub>	9.6	18.6	230	[31]
Gd <sub>2</sub> NiSi <sub>3</sub>	16	13	233	[32]
Tm <sub>2</sub> Cu <sub>2</sub> In	39.4	14.4	331	[33]
Ho <sub>2</sub> Co <sub>2</sub> Ga	38.5	11.7	271	[34]
Dy <sub>11</sub> Co <sub>4</sub> In <sub>9</sub>	37	3.53	128.4	[35]

## 4. Conclusions

To summarize, the magnetic transitions and MCE performances of the biphasic HoNi/HoNi<sub>2</sub> composite were studied in detail. Two crystalline phases HoNi and HoNi<sub>2</sub> have been identified with the weight ratios of 52.4 wt.% and 47.6 wt.%, respectively. The magnetization measurements indicated that the composite undergoes three successive magnetic transitions at 13 K, 16 K, and 38.5 K, respectively. The table-like shape MCE was achieved in HoNi/HoNi<sub>2</sub> composite because of the proper distribution of transition temperatures and the  $-\Delta S_M$  values with similar magnitude of the phases, which make it appropriate for the Ericsson type magnetic refrigeration cycle. The values of  $-\Delta S_M^{\max}$  are 14.93 J/(kg·K) and 18.23 J/(kg·K)

for  $\Delta H = 0\text{--}50$  kOe and  $0\text{--}70$  kOe, respectively. In addition, for the  $\Delta H$  of  $0\text{--}50$  kOe, the  $RC_1$ ,  $RC_2$ , and  $RC_3$  are 623.5 J/kg, 469.2 J/kg, and 342.4 J/kg, respectively.

## References

- [1] Franco V, Blázquez J S, Ipus J J, Law J Y, Moreno-Ramírez L M and Conde A 2018 *Prog. Mater. Sci.* **93** 112
- [2] Li L W and Yan M 2020 *J. Alloys Compd.* **823** 153810
- [3] Zhang Y K 2019 *J. Alloys Compd.* **787** 1173
- [4] Zhang Y K, Guo D, Wu B B, Wang H F, Guan R G and Ren Z M 2020 *J. Appl. Phys.* **127** 033905
- [5] Zhang B, Zheng X Q, Zhao T Y, Hu F X, Sun J R and Shen B G 2018 *Chin. Phys. B* **27** 067503
- [6] Tang B Z, Liu X P, Li D M, Yu P and Xia L 2020 *Chin. Phys. B* **29** 056401
- [7] Pecharsky V K and Gschneidner Jr K A 1997 *Phys. Rev. Lett.* **78** 4494
- [8] Liu J, Gottschal T, Skokov K, Moore J and Gutfleisch O 2012 *Nat. Mater.* **11** 620
- [9] Jiang W H, Mo Z J, Luo J W, Zheng Z X, Lu Q J, Liu G D, Shen J and Li L 2020 *Chin. Phys. B* **29** 037502
- [10] Tegus O, Brück E, Buschow K H J and de F R 2002 *Nature* **415** 150
- [11] Wu X F, Guo C P, Cheng G, Li C R, Wang J, Du Y S, Rao G H and Du Z M 2019 *Chin. Phys. B* **28** 057502
- [12] Li L W 2016 *Chin. Phys. B* **25** 037502
- [13] Li L W, Xu P, Ye S K, Li Y, Liu G D, Huo D X and Yan M 2020 *Acta Mater.* **194** 354
- [14] Ghosh S, Sen P and Mandal K 2020 *J. Magn. Magn. Mater.* **500** 166345
- [15] Yang L, Liu J, Zhou Z N, Zhang R Y, Tu D F, Hu Q D, Dong H B and Li J G 2020 *J. Alloys Compd.* **817** 152694
- [16] Miao X F, Wang W Y, Liang H X, Qian F J, Cong M Q, Zhang Y J, Muhammad A, Tian Z J and Xu F 2020 *J. Mater. Sci.* **55** 6660
- [17] Zheng X Q, Chen J, Wang L C, Wu R R, Hu F X, Sun J R and Shen B G 2014 *J. Appl. Phys.* **115** 17A905
- [18] Ibarra-Gaytán P J, Sánchez Llamazares J L, Álvarez-Alonso P, Sánchez-Valdés C F, Gorria P and Blanco J A 2015 *J. Appl. Phys.* **117** 17C116
- [19] Li L W, Niehaus O, Kersting M and Pöttgen R 2014 *Appl. Phys. Lett.* **104** 092416
- [20] Li L W, Namiki T, Huo D X, Qian Z H and Nishimura K 2013 *Appl. Phys. Lett.* **103** 222405
- [21] Chaturvedi A, Stefanoski S, Phan M H, Nolas G S and Srikanth H 2011 *Appl. Phys. Lett.* **99** 162513
- [22] Álvarez P, Sánchez Llamazares J L, Gorria P and Blanco J 2011 *Appl. Phys. Lett.* **99** 232501
- [23] Li L W, Yuan Y, Qi Y, Wang Q and Zhou S Q 2018 *Mater. Res. Lett.* **6** 67
- [24] Zhou H Y and Ou X L 1991 *J. Alloys Compd.* **177** 101
- [25] Ćwik J, Koshkid'ko Y, Nenkov K, Tereshina E A and Rogacki K 2018 *J. Alloys Compd.* **735** 1088
- [26] Zheng X Q, Zhang B, Wu H, Hu F X, Huang Q Z and Shen B G 2016 *J. Appl. Phys.* **120** 163907
- [27] Rajivgandhi R, Arout Chelvane J, Quezado S, Malik S K, Nirmala R 2017 *J. Magn. Magn. Mater.* **433** 169
- [28] Legvold S 1980 *Handbook of Ferromagnetic Materials* (Amsterdam: North-Holland Publishing Company) p. 183
- [29] Banerjee B K 1964 *Phys. Lett.* **12** 16
- [30] Zhang Y K, Guo D, Wu B B, Wang H F, Guan R G, Li X and Ren Z M 2020 *J. Alloys Compd.* **817** 152780
- [31] Kadim G, Masrour R, Jabar A 2020 *J. Magn. Magn. Mater.* **499** 166263
- [32] Pakhira S, Mazumdar C, Ranganathan R, Giri S and Avdeev M 2016 *Phys. Rev. B* **94** 104414
- [33] Zhang Y K, Yang Y, Xu X, Hou L, Ren Z M, Li X and Wilde G 2016 *J. Phys. D: Appl. Phys.* **49** 145002
- [34] Zhang Y K, Guo D, Geng S H, Lu X G and Wilde G 2018 *J. Appl. Phys.* **124** 043903
- [35] Zhang Z Q, Wang P Y, Wang N, Wang X J, Xu P and Li L W 2020 *Dalton Trans.* **49** 8764